Seventh Symposium on Salt, Vol. II 123–130 (1993)
Elsevier Science Publishers B.V., Amsterdam

Correlation between Product Crystal Size and Productivities of Sodium Chloride Crystals in a Continuous Classified Bed Crystallizer

Ken Toyokura[1], Izumi Hirasawa[1], Masanori Minozaki[1], Yoshinobu Tanaka[2], Masami Hasegawa[2], Leo Ehara[3], Atsushi Ohtsubo[3], Isao Ogura[4], Tohru Kageyama[4], Yoshihiro Yamaguchi[5], Kouichi Nishioka[5], Tomio Shimomura[6], Michihiko Nakamura[6], Yasuzi Nishino[7], Shinichi Hayashi[7], Noboru Miyatake[8], Masahiro Ishikawa[8] and Takaomi Tsukamoto[9]

[1]*Waseda University, Japan*
[2]*Japan Tobacco Inc., Japan*
[3]*Shin Nihon Chem. Ind. Co., Japan*
[4]*Ako Seawater Ind. Co. Ltd., Japan*
[5]*Kinkai Engyo Co. Ltd., Japan*
[6]*Naikai Engyo Co. Ltd., Japan*
[7]*Naruto Engyo Co. Ltd., Japan*
[8]*Sanuki Engyo Co. Ltd., Japan*
[9]*Sakito Seien Co. Ltd., Japan*

ABSTRACT

Crystallization of sodium chloride in seven different industrial crystallizers and in one laboratory crystallizer were studied. The industrial crystallizers were 45–120 m^3 in actual volume and the laboratory one was 5.80×10^{-4} m^3. In these studies, the production rate was observed and, when operation became steady, the size distribution of the crystals produced was measured by sieving and plotted in the Rosin–Rammler diagram. From these data, a representative product size and a uniformity of size distribution were obtained for individual operational conditions and the product crystal size (l_w) was plotted against productivity of sodium chloride ($P/\varrho_c V'$) in the design chart proposed by Toyokura. Operating points shown by $P/\varrho_c V'$ and l_w were divided into two groups characterized by their slopes. Experiments in a continuous laboratory crystallizer were carried out under operating suspension volume 1.08×10^{-4} to 2.02×10^{-4} m^3, and correlation between $P/\varrho_c V'$ and the dominant size l_d were obtained. The correlative lines differed for cases with and without increasing the temperature of recirculation flow. The correlative lines from laboratory data were reasonably compared with that of some industrial crystallizers. Average effective nucleation rate and crystal growth rate were estimated from these data obtained in industrial and laboratory crystallizers and discussed with respect to the type and size of the crystallizer. The design of industrial crystallizers for sodium chloride is also discussed from obtained correlative lines.

INTRODUCTION

Design theories for continuous crystallizers have been studied and applied to many systems (Aoyama et al., 1988). Engineers from eight Japanese salt manufacturing companies set up a working party to study the crystallization of sodium chloride in industrial crystallizers and to discuss data concerning industrial operations and design theory. From these studies, correlations between product crystal size and the productivity of sodium chloride crystals are proposed on the design chart (Toyokura and Sakai, 1987) for two different types of operation of continuous fluidized bed crystallizers, and compared with those obtained from laboratory test data. As the result of this study, an idea for the development of a new type of crystallizer is proposed from the crystal nucleation rate and growth one.

THEORETICAL BACKGROUND

Production rate, P, and product crystal size distribution on steady-state operations of continuous crystallizers are important for the evaluation of

capacities of crystallizers, and equations (1) and (2) are proposed (Toyokura and Sakai, 1987):

$$P = \varrho_c \int_0^\infty k_v f(l_p) l_p^3 dl_p \quad (1)$$

$$R = \exp\{-(l_p/l^*)^m\} = \int_{l_p}^\infty f(l_p)dl_p / \int_0^\infty f(l_p)dl_p \quad (2)$$

where k_v and $f(l_p)$ are volumetric shape factor and population of crystal of size l_p in product crystal; R is the relative cumulative number of product crystal larger than l_p and correlated by Rosin–Rammler equation; l^* and m are particular crystal size at R = 0.3677 and uniformity number which is a slope of a plotted line in the Rosin–Rammler diagram. When the crystal size distribution of weight basis is expressed by the particular crystal size l_w or dominant size l_d and uniformity number n, l_d is correlated by equation (3) and l_w, or n is correlated with l_d and m, or n as the line in Figs. 1 or 2, respectively.

$$l_d = \left(1 + \frac{2}{m}\right)^{1/m} l^* \quad (3)$$

From equations (1) and (2) for P and $R(l_p)$, correlative equations (4) and (5) are derived.

$$P/\varrho_c V' = l^{*3}\left\{F_v' k_m m \int_0^\infty x^{m+2} e^{-x^m} dx\right\} \quad (4)$$

$$P/\varrho_c V' = \{(1-\varepsilon)(dl/dt)_{av}/l^*\}\left\{\int_0^\infty e^{-x^m}dx \int_0^\infty x^{m+2}e^{-x^m}dx/\right.$$

$$\left.\left\{\int_0^\infty x^m e^{-x^m}dx \int_0^\infty x^3 e^{-x^m}dx\right\}\right. \quad (5)$$

Here, V', ϱ_c, F_v', $(1-\varepsilon)$, $(dl/dt)_{av}$. are volume of a crystallizer, density of crystal, average nucleation rate in a unit volume of a crystallizer, average volumetric suspension density of crystals in a crystallizer, average growth rate of crystals suspended in a crystallizer, respectively. Equations (4) and (5) give the correlation between $P/\varrho_c V'$, l_w (or l_d), $F_v' k_v$, $(1-\varepsilon)$, $(dl/dt)_{av}$ and m and a particular operating point expressed by $P/\varrho_c V'$ and l_w(or l_d) is plotted on the design chart in Fig. 3, derived from these equations. This particular operating point is also decided by two of the following four terms: l_w (or l_d), $P/\varrho_c V'$, $F_v' k_v$ and a set of l_w(or l_d) and $(1-\varepsilon)$. When particular operating points are plotted from data obtained under the same suspension density of crystal in the same type of crystallizer, they are on a straight line, independent of the size of crystallizer; the straight line is the particular operating line restricted to the system, type of crystallizer and operating suspension density. When a particular line is obtained by laboratory tests, industrial crystallizers are considered to be easily designed.

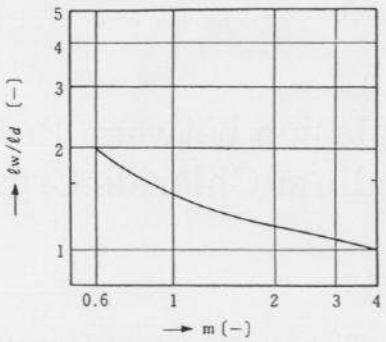

Fig. 1. Correlation between l_w/l_d and m.

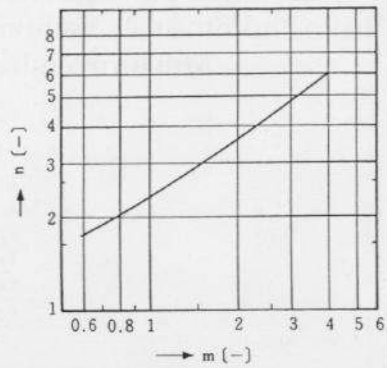

Fig. 2. Correlation between n and m.

CRYSTALLIZATION OF SODIUM CHLORIDE IN CONTINUOUS INDUSTRIAL CRYSTALLIZERS

Seven industrial crystallizers were used, classified into two different types. The difference between the two types was in the circulation flow of the solution, as shown in Fig. 4. In type A, the evaporator was separated from the crystallizer and the concentrated solution from the evaporator was divided into two flows: one was fed into the crystallizer for crystal growth and the other was added to the flow of the solution flooded from the crystallizer; the mixed solution then flowed into a heat exchanger. In type B crystallizers, evaporation occurred on the upper surface of the solution in the crystallizer and the concentrated solution with some fines was flooded from the crystallizer and returned

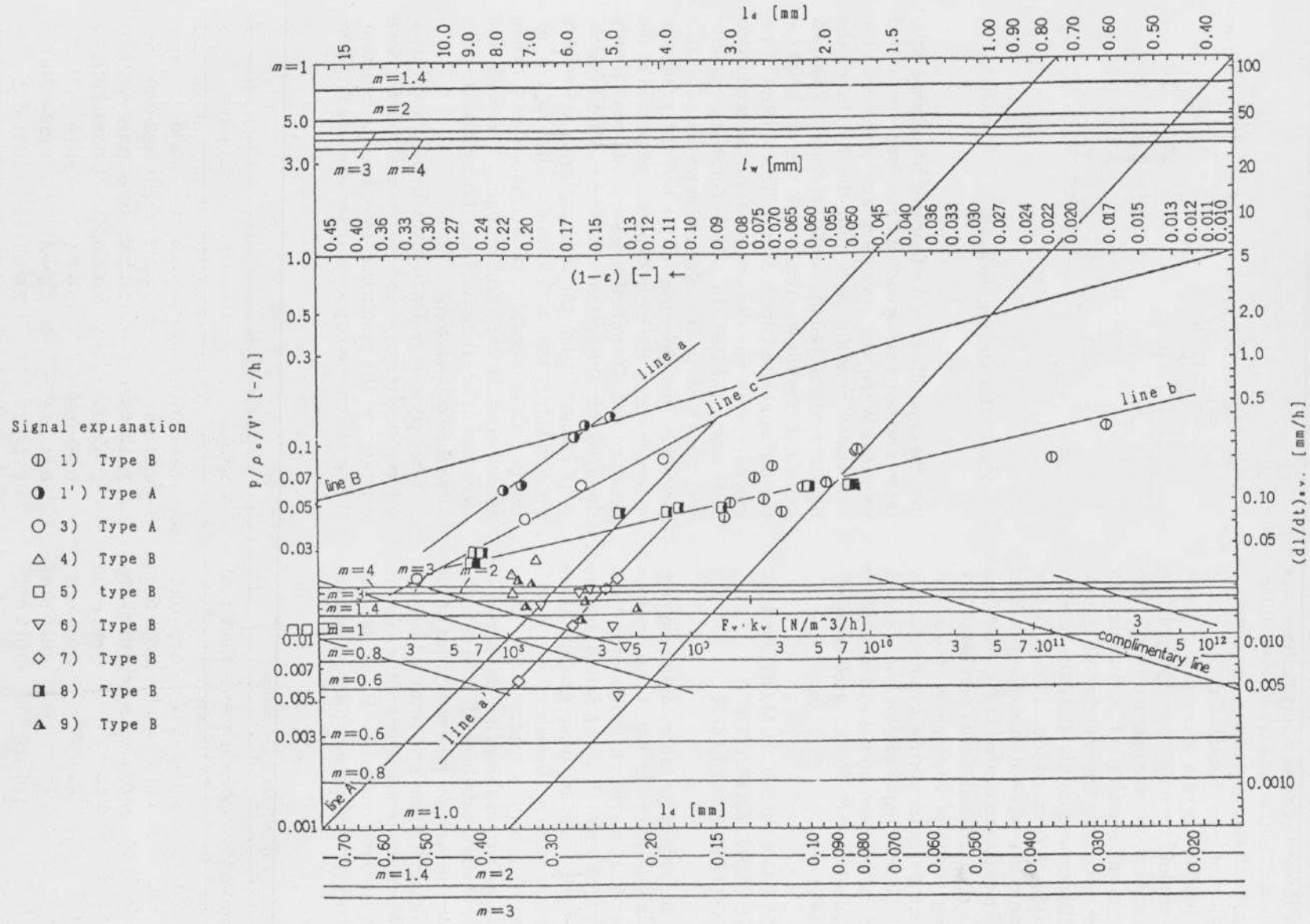

Fig. 3. Correlation between $P/\rho_0/V'$, l_d (or l_w), $F_v k_v$, m, $(1-\varepsilon)$ and $(dl/dt)_{av}$. 1,1': Laboratory tests by Waseda University; 3–9: authors' companies.

back through a heat exchanger. Therefore, the effective nucleation rate in a type A crystallizer was supposed to be less than that in a type B crystallizer even when the growth rate was almost the same.

These crystallizers were operated under steady states and the production rate of crystals and size distribution of product crystals were observed. The observed size distributions were plotted in a Rosin–Rammler diagram and crystal size l_w and uniformity number n were obtained. The volumes of the industrial crystallizers used in this study are listed in Table 1 with ranges of observed data of $P/\varrho_c V'$, l_w and n. The operating points of a continuous crystallizer shown by $P/\varrho_c V'$ and l_w, are plotted in Fig. 3 for data from operations of individual plants numbered 3 to 9. The operating points of these plots are roughly divided in two groups, characterized by lines c and b. When lines c and b are compared with line A and B, the slope of line c is between lines A and B, and line b is nearly parallel to line B. These correlations will be discussed later.

CRYSTALLIZATION OF SODIUM CHLORIDE IN A CONTINUOUS LABORATORY FLUIDIZED BED CRYSTALLIZER

A schematic diagram of the laboratory equipment used in this study is shown in Fig. 5. An aqueous solution saturated at a desired temperature was prepared in the feed tank (1). This solution was fed into an evaporator (2), kept at a desired temperature and became supersaturated. Details of the crystallizer are shown in Fig. 5 and a supersaturated solution was fed to the bottom through a down-pipe in the central part of the crystallizer (6). The solution was flooded from the overflow pipe positioned at the upper part of the crystallizer and returned back to the feed tank. When the temperature of the solution became steady, the seed crystal — whose size distribution had been previously observed — was fed

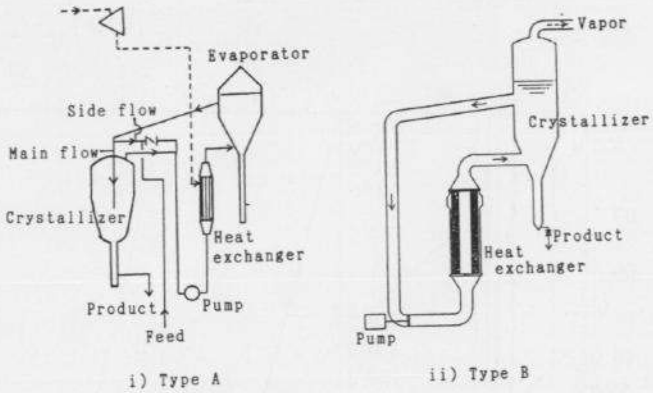

Fig. 4. Schematic diagram of industrial crystallizer.

into the crystallizer and a fluidized bed of seed crystal was made by an ascending flow of supersaturated solution. When the operation was continued, the suspended crystals grew and the height of the fluidized crystal bed gradually increased. Then, an amount of crystals was removed so that the height of the bed might be kept constant. The amount of removed crystals was also observed and the production rate was estimated. In these operations, smaller crystals, grown from nuclei, are supposed to be suspended in the upper part of the bed and gradually moved down by the hydrodynamic properties of the fluidized bed. Classified large crystals were finally fluidized into the bottom of the bed. When crystals were removed from the bottom, larger ones were predominantly removed. Therefore, during the initial periods of operation, those crystals grown from seeded crystals were predominantly removed, and were completely removed from the crystallizer after some time of operation.

When crystals grown from nuclei born in the crystallizer were removed and the removal rate of grown crystals, i.e. the production rate, became constant, the operation was supposed to become steady. Then,

TABLE 1

Ranges of data obtained by industrial crystallizer

Type	Company*	V′ (m^3)	$P/\varrho_c V'$ (–/h)	l_w (mm)	n (–)	$1-\varepsilon$ (–)
A	3	–	0.02–0.085	1.14–2.00	4.8–6.2	0.30
B	4	61	0.016–0.0256	1.25–1.31	2.7–3.5	0.25–0.40
B	5	140	0.0113–0.015	2.45–2.60	2.5–3.5	0.219
B	6	60	0.018–0.049	0.54–1.05	2.9–5.0	0.039–0.078
B	7	85	0.006–0.02	0.082–0.88	5.4–6.1	0.10
B	8	45	0.025–0.061	0.44–1.78	3.5–4.8	0.012–0.316
B	9	110–120	0.013–0.02	0.71–1.29	2.8–4.1	0.11–0.23

*See page 123 for the company name of each author represented by these numbers.

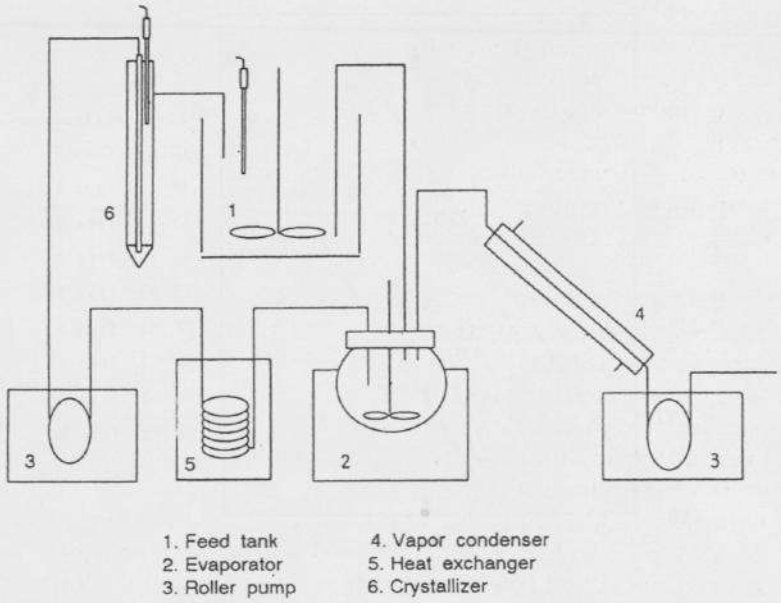

Fig. 5. Schematic diagram of the laboratory equipment.

TABLE 2

Data from the laboratory tests

Test	Run	V' (m^3)	$P/\varrho_c V'$ (–/h)	l^*(mm)	m (–)	$1-\varepsilon$ (–)
1	1	108.0	0.0937	0.48	4.65	0.180
	2	141.5	0.0610	0.54	6.47	0.193
	3	174.0	0.0453	0.54	5.84	0.241
	4	108.0	0.0776	0.64	5.07	0.272
	5	141.5	0.0506	0.66	4.38	0.278
	6	174.0	0.0417	0.62	4.35	0.270
	7	108.0	0.0843	0.19	3.46	0.133
	8	141.5	0.0655	0.49	5.26	0.153
	9	174.0	0.0526	0.59	4.35	0.266
	10	108.0	0.1282	0.17	3.16	0.0480
	11	141.5	0.0957	0.49	5.03	0.140
	12	174.0	0.0694	0.64	3.74	0.207
1′	1	202.1	0.0658	1.78	8.55	0.291
	2	202.1	0.0597	1.88	9.65	0.286
	3	139.2	0.1411	1.59	7.56	0.384
	4	139.2	0.1098	1.72	7.68	0.321
	5	139.2	0.1267	1.74	10.0	0.286

the crystal production rate P, volume of a fluidized bed V', suspension density of crystal $(1-\varepsilon)$, and crystal size distribution were observed. The observed size distribution was plotted on a Rosin–Rammler diagram and crystal size l^* and uniformity number m were obtained. The volume of the fluidized bed of crystals was estimated from observation of the height of the bed. These data are listed in Table 2 with operating conditions. Tests noted by run number from 1′–1 to 1′–5 were carried out through the method whereby the solution in the feed tank was heated to dissolve the fine sodium chloride crystals in the solution flooded from the crystallizer. In tests of run number 1–1 to 1–12, the temperature of the solution in the feed tank was almost equal to that in the crystallizer and fines from the crystallizer were circulated without dissolution. Productivity $P/\varrho_c V'$ estimated from observed data, are plotted in Fig. 3 against crystal size l_d estimated from the size distribution plot in a Rosin–Rammler diagram. The data of test run numbers 1–1 to 1–12 were plotted near the line obtained by the test data from the type B industrial crystallizer 8 and the extrapolated one. The slope of a line fitted with plots from data of test run numbers 1′–1 to 1′–5 was larger than that of the line obtained by test data of type A industrial crystallizer 3 and close to that of line A.

DISCUSSION

Average nucleation rates and crystal growth rates

Average nucleation and crystal growth rates in a crystallizer are easily obtained from the plots in Fig. 3, as follows: a vertical line is drawn from an operating point and crosses the axis of $F_v k_v$ of m = 1. The line parallel to the complementary line drawn from the cross point gives a complementary point as a cross point on the axis of $F_v k_v$ particularized by a

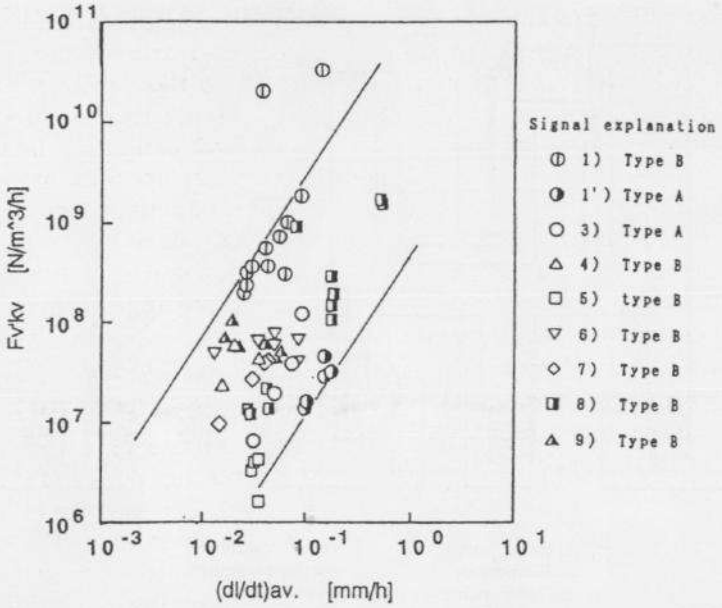

Fig. 6. Correlation between nucleation rate and average crystal growth rate.

slope of a line of size distribution plotted in a Rosin–Rammler diagram m. When a complementary point is read by the axis of $F_v k_v$ of m = 1 an average modified nucleation rate is obtained. Also, a line parallel to line B from an operating point decides the secondary operating point by $(1 - \varepsilon)$ and an average crystal growth rate is obtained from the secondary operating point by $(dl/dt)_{av.}$ axis. Average modified nucleation and crystal growth rates obtained from data in Table 2 are listed in Table 3 and plotted in Fig. 6. The plots of nucleation rates of the test run 1′ group are much less than those of the test run 1 group and it is supposed that these differences come from the dissolution of fines in feed tank 1 on test run 1′. These rates in industrial crystallizers, also calculated from data in Table 1 and Fig. 3, are shown by the range in Table 4 and plotted in Fig. 6. Data from industrial crystallizers are between those of laboratory test run 1′ and those of test run 1. Supersaturation is generally supposed to affect nucleation rate more than crystal growth rate and the size of the crystallizer is considered to affect the average super-

TABLE 3

Average modified nucleation and growth rate in laboratory tests

Test	Run	$(dl/dt)_{av.}$ (μm/h)	$F_v k_v$ (N/h·m^3)
1	1	65	1.0E9
	2	40	5.5E8
	3	26	3.2E8
	4	42	3.5E8
	5	26	2.3E8
	6	25	2.0E8
	7	38	2.0E10
	8	55	7.0E7
	9	28	3.5E8
	10	140	3.2E10
	11	90	1.8E9
	12	62	3.0E8
1′	1	102	1.6E7
	2	95	1.4E7
	3	147	4.6E7
	4	149	3.0E7
	5	178	3.3E7

TABLE 4

Average modified nucleation and growth rate in industrial crystallizer

Company*	$(dl/dt)_{av.}$ (μm/h)	$F_v k_v$ (N/h·m^3)
3	30–90	6.4E6–1.2E8
4	20–33	2.3E7–6.0E7
5	28–34	1.6E6–4.3E6
6	13–82	4.0E7–7.8E7
7	14–45	9.0E7–4.0E7
8	27–190	1.2E7–1.7E9
9	16–58	4.3E7–1.0E8

saturation in the crystallizer. Plots of data from industrial crystallizers in Fig. 6 differ between crystallizers even though the average crystal growth rates are not much different, and are considered to result from the difference in the size of the crystallizers.

Operating points defined by $P/\varrho_c V'$ and l_d or l_w

Characteristics of operating points defined by $P/\varrho_c V'$ and l_d or l_w are expressed by equations (3), (5) and Fig. 1. When $(P/\varrho_c V')l^*$, [or $(P/\varrho_c V')l_d$, $(P/\varrho_c V')l_w$] is constant a correlative line between $P/\varrho_c V'$ and l_w (or 1^*, l_d) becomes parallel to line B in Fig. 3. Plots of the data obtained from industrial crystallizer 8 are on the straight line b parallel to line B, and line b is also fitted for data of laboratory test run 1. Although the volume of industrial crystallizer 7 is about 3×10^5 times of that of a laboratory crystallizer used in test run 1, the correlative line is considered to be almost same.

Data from laboratory test run 1′ or from industrial test run 7 is closely plotted on the line parallel to line A. In these operations the solution flooded from the crystallizer is supposed to be almost free from fines because in the laboratory tests the solution was heated up to be unsaturated, and supersaturation on test run 7 is supposed to be very small, since productivities were much lower than those from other operations. In these cases, average nucleation rates per unit volume of the crystallizer are supposed to be proportional to productivities and also to $(1-\varepsilon)(dl/dt)_{av.}$; these correlations are almost the same as those reported by Aoyama (Aoyama, 1982). These correlations are considered to be affected by the system and the type of crystallizer.

Plots of data obtained from industrial crystallizer 3 are correlated as equation (6):

$$P/\varrho_c V' = 0.135\,(l_w)^{-2.60} \qquad (6)$$

where l_w is the particular crystal size of weight basis (mm).

Slopes of the correlative lines in Fig. 3 are between the slope of the lines a and a′ and those of line b. The difference between the slopes of these lines are supposed to be due to partial dissolution of fines during operations.

Other industrial data are plotted below line b in Fig. 3 and are supposed to result from the difference between evaporation rate per unit volume of crystallizers, suspension densities, superficial velocities of circulation flow, type of pump etc. Although the data from different industrial crystallizers are insufficient to be discussed in details (because of the company circumstances), these data are plotted within a reasonable range in the diagram of Fig. 3.

When crystallization data of a particular type of crystallizer are obtained, the operating points are plotted on the design chart in Fig. 3. From these points reasonable productivity in the same type of crystallizer can easily be decided for a desired product crystal size. The operational conditions for estimated productivity and crystal size are also decided from a suspension density, and the average effective nucleation and growth rate corresponding to an estimated operating point.

CONCLUSIONS

Crystallization of sodium chloride was studied in industrial and laboratory continuous crystallizers, and operating points of $P/\varrho_c V'$ and crystal size were obtained. The average effective nucleation rate and crystal growth rate were estimated from operating points and discussed with respect to the type and size of crystallizers. Operating points obtained from different types and sizes of crystallizers are also discussed with respect to industrial application and operational conditions for a desired product are proposed which can be ascertained by using a design chart.

ACKNOWLEDGEMENT

This study was supported by Salt Research Scientific Fund no. (900A-1) for which we record our appreciation.

NOMENCLATURE

- P production rate ($kg\cdot h^{-1}$)
- k_v volumetric shape factor (–)
- l_p product crystal size (m)
- $f(l_p)$ population of product crystal size l_p ($N\cdot h^{-1}\cdot m^{-1}$)
- R relative cumulative number of product crystal larger than l_p (%)
- l^* particular crystal size at R = 0.3677 (m)
- m uniformity number expressed by a slope of crystal population on the Rosin–Rammler diagram (–)
- l_w particular crystal size of weight basis (m)
- l_d dominant crystal size of weight basis (m)
- n uniformity number of crystal weight basis (–)
- V' volume of a crystallizer (m^3)
- $F_{v'}$ nucleation rate in a unit volume of a crystallizer ($N\cdot m^{-3}\cdot h^{-1}$)
- $(1-\varepsilon)$ volumetric suspension density of crystal in crystallizer (–)
- $(dl/dt)_{av.}$ average growth rate of crystal suspended in a crystallizer ($m\cdot h^{-1}$)
- ϱ_c density of crystal ($kg\cdot m^{-3}$)